



Structure Effect on Reflective Gyrotron Backward-Wave Oscillator

Chia-Chuan Chang(張家鈞)¹, Tien-Fu Yang(楊添福)¹, Hsin-Yu Yao(姚欣佑)², Tsun-Hsu Chang(張存績)¹

¹Department of Physics, National Tsing Hua University, Hsinchu, Taiwan

²Department of Physics, National Chung Cheng University, Chiayi, Taiwan

Email: cc1141596063@hotmail.com

Abstract –gyrotron devices, based on the principles of the electron cyclotron maser (ECM) instabilities, are powerful high-frequency microwave sources. In this study, we focus on specific type of reflective type gyro-BWO, which consist of several tapered section and can achieve a phenomenal output efficiency and bandwidth. This study investigates the effect of structural nonuniformities on the beam-wave interactions in the gyrotron backward-wave oscillator (gyro-BWO). Employing the effective-boundary method both upstream and downstream of the primary cavity, we examine the modulation effect resulting from end reflections. The gyrotron's beam-wave dynamics during backward wave and forward wave interactions are analyzed separately. The study reveals a significant modulation effect during the electron bunching stage of backward-wave interaction, influencing tunability positively or negatively. This modulation effect is contingent upon the acquired phase from upstream reflections. The influence of both upstream and downstream structural nonuniformities is elucidated. These findings not only provide valuable insights but also offer a clear physical understanding for optimizing current gyrotron devices.

I. Introduction and motivation

Gyrotron backward-wave oscillator (gyro-BWO), featuring continuous and smooth frequency tuning in a non-resonant structure (internal feedback), is capable of stable operation in the nonlinear region with fine frequency tunability and high power. However, the absence of a terahertz mode converter for extracting wave energy at the beam entrance has led to interest in converter-free, reflective-type gyro-BWOs (R-gyro-BWOs). These R-gyro-BWOs, resembling the gyrotron in delivering wave power forward, have sparked interest. Nevertheless, the characteristic of the R-gyro-BWO seems not well understood to date and it tends to be ambiguous with that of the low power gyrotron. They do have analogous configurations in interaction structure, but the working mechanisms as well as design principles are studied from the distinct perspectives: beam-wave resonance and structure resonance. To better comprehend the linear and nonlinear properties of a frequency-tunable gyrotron, a general principle applied for both the R-gyro-BWO and the low power gyrotron is pressingly desired.

II. Model and Simulation Parameters

(A) Interaction Structure and Beam Parameters

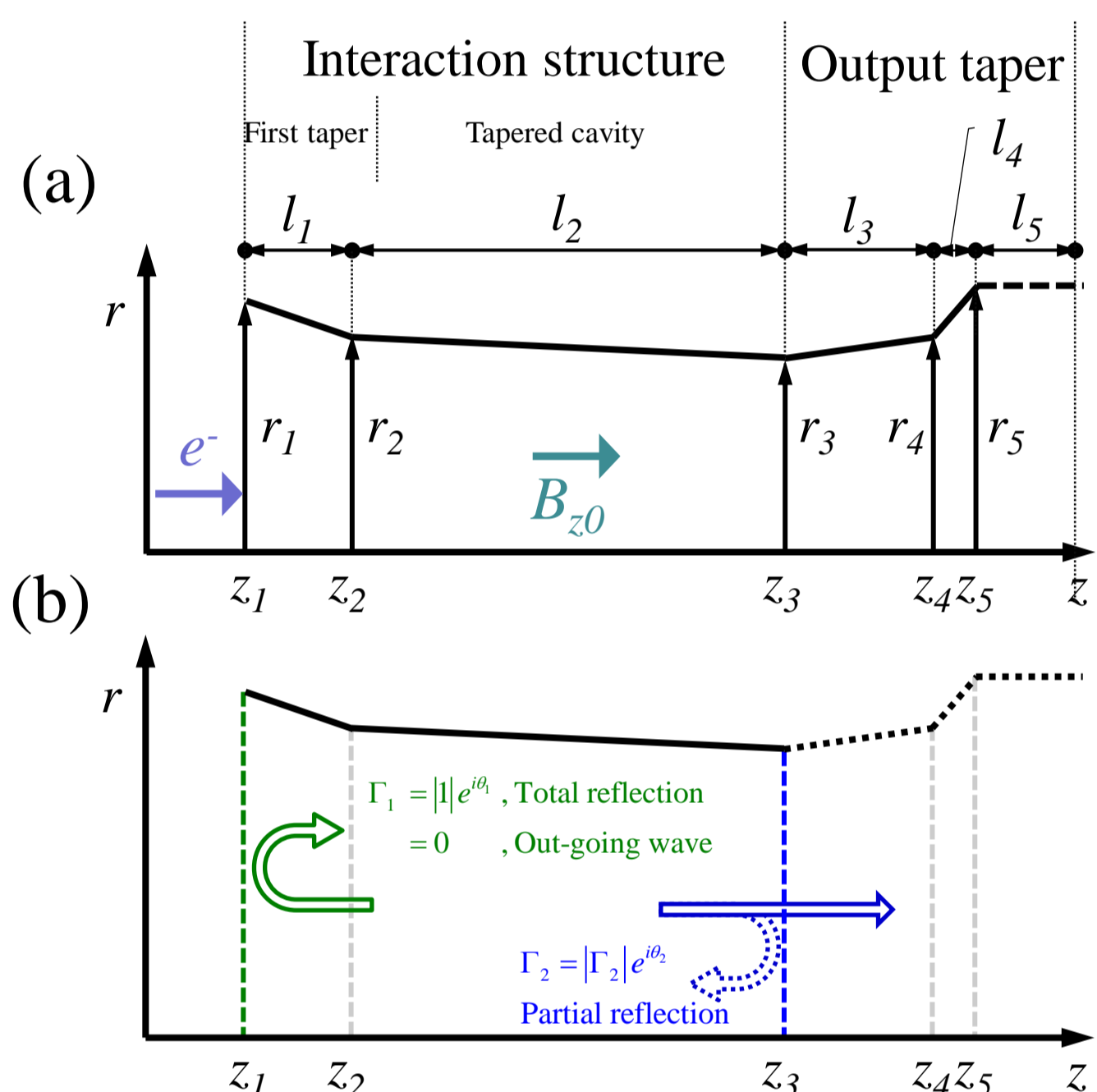


Table 1. Dimension of interaction structure.

Position(cm)	Length(cm)	Radius(cm)	Angle(Deg)
z_1	l_1	r_1	0.179
z_2	l_2	r_2	0.172
z_3	l_3	r_3	0.168
z_4	l_4	r_4	0.1718
z_5	l_5	r_5	0.182

Table 2. Electron and wave parameters

Parameter	Symbol	Value	Unit
Mode		TE ₀₂ ⁽¹⁾	
Beam Voltage	V_b	25	kV
Beam Current	I_b	0.5	A
Velocity Ratio	a	1.5	
Guiding Center	r_c	0.0442	cm
Velocity Spread	$\Delta v_z/v_z$	0.0	%
Magnetic Field	B_{z0}	7.6-8.1	T

Fig. 1. Radius (r) vs position (z). A total reflection B.C. at left boundary for R-gyro-BWO; An outgoing-wave B.C. at left boundary for gyro-BWO. (a) Normal model: Out-going wave B.C. at right boundary. (b) Effective model: Truncate the structure at z_3 and apply effective B.C. for structure reflection. The output power in Section III(A) was sampled at $z = z_3$ on both models.

(B) Initial Assignment and End Discriminant of Wave Equation

The Wave Equation

$$f(z) = f_+(z)e^{ik_z z} + f_-(z)e^{-ik_z z},$$

Decompose when f is weak dependence of z

$$f_- \cong \frac{ik_{zr} f - f'}{2ik_{zr}} e^{+ik_{zr} z}, f_+ \cong \frac{ik_{zr} f + f'}{2ik_{zr}} e^{-ik_{zr} z}$$

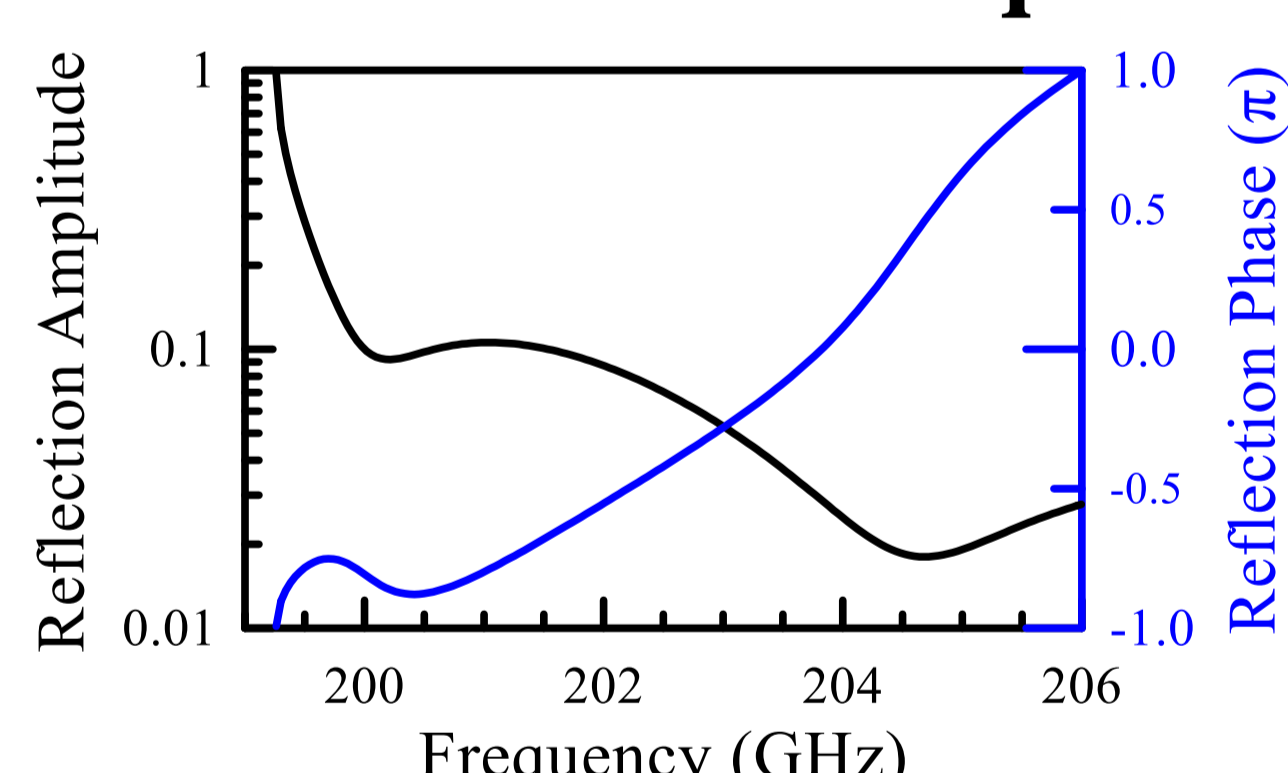
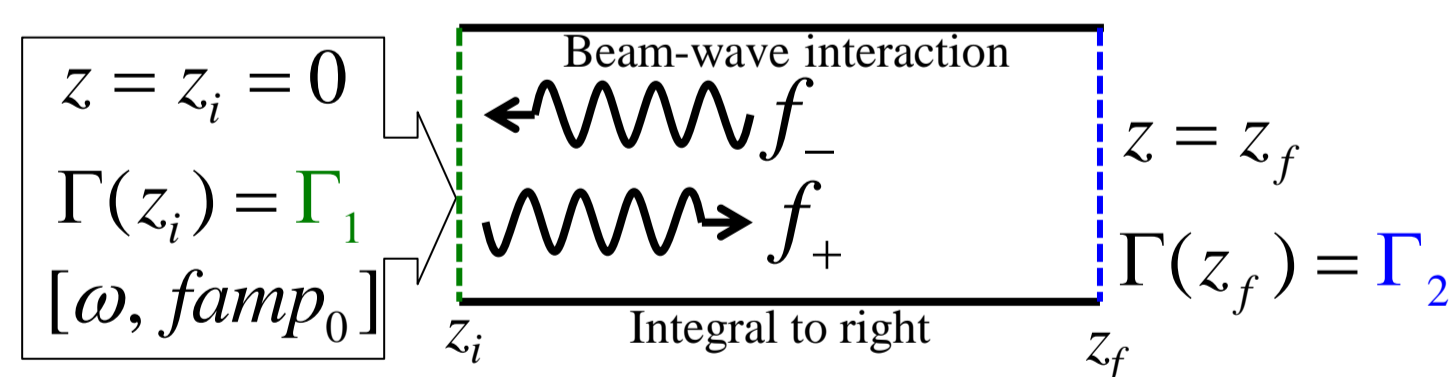


Fig. 2. Calculated reflection amplitude and phase at $z = z_3$ of output end $\Gamma_2 = |\Gamma_2| e^{i\theta_2}$ by single mode frequency domain simulation.



Initial Assignment

$$f(z_i) = famp_0 (\Gamma_1 e^{ik_z(z_i)z_i} + e^{-ik_z(z_i)z_i})$$

$$f'(z_i) = ik_z famp_0 (\Gamma_1 e^{ik_z(z_i)z_i} - e^{-ik_z(z_i)z_i})$$

Effective Reflection B.C. $\Gamma_1 = |1| e^{i\theta_1}$ Outgoing-Wave B.C. $\Gamma_1 = 0$

End Discriminant

Effective Reflection B.C.

$$D(\omega, famp_0) = \Gamma_2 - \frac{ik_{zr} f - f'}{ik_{zr} f + f'} = 0$$

Outgoing-Wave B.C.

$$D(\omega, famp_0) = ik_{zr} f - f' = 0$$

III. Simulated Results

(A) Structure Effect Of Output Taper

An intuitive difference between normal and effective model is that they might have different feedback power due to additional beam-wave interaction. This part investigates the relation between feedback power (sampled at $z = z_3$) and overall efficiency.

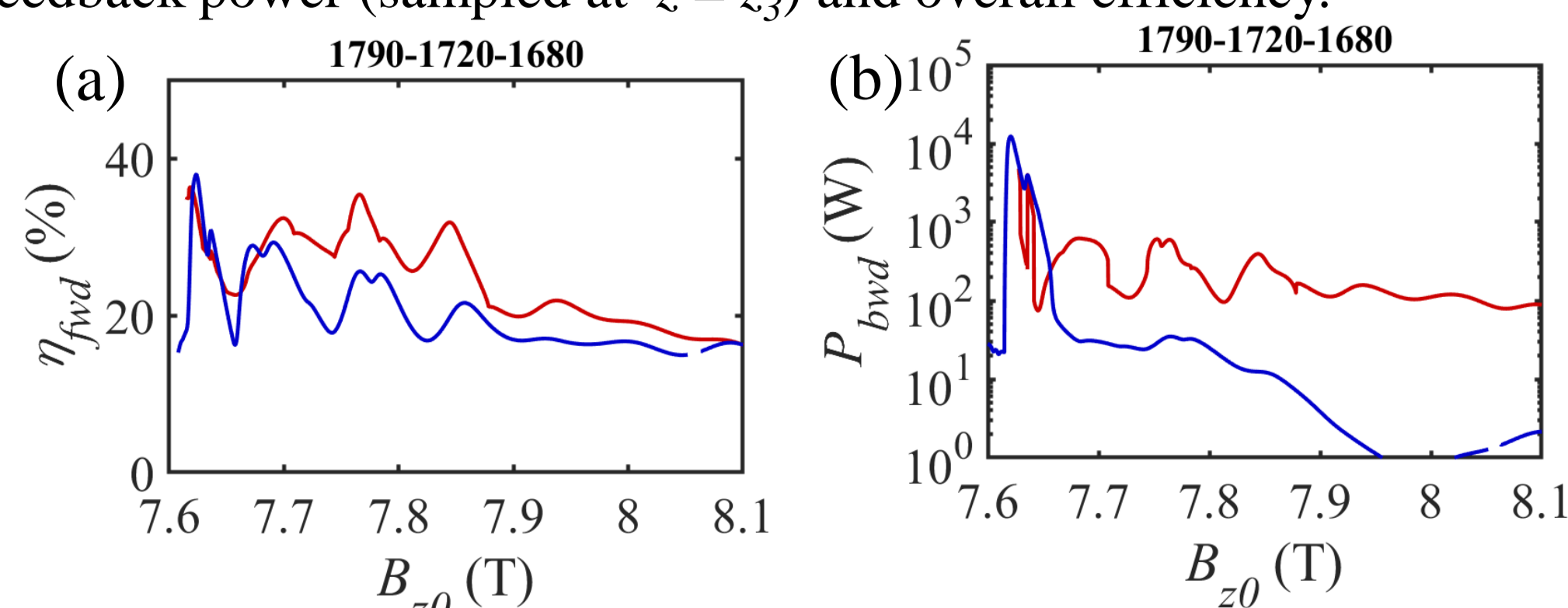


Fig. 3. Simulated result of two model, red line and blue line represent normal model and effective model respectively. (a) Forward wave efficiency vs magnetic field. (b) Feedback power at $z = z_3$ of output end two stage output taper end.

Feedback enhancement
The downstream taper effect is an extension that improves the efficiency and bandwidth of the main interaction in the low frequency region.

(B) Structure Effect Of First Taper

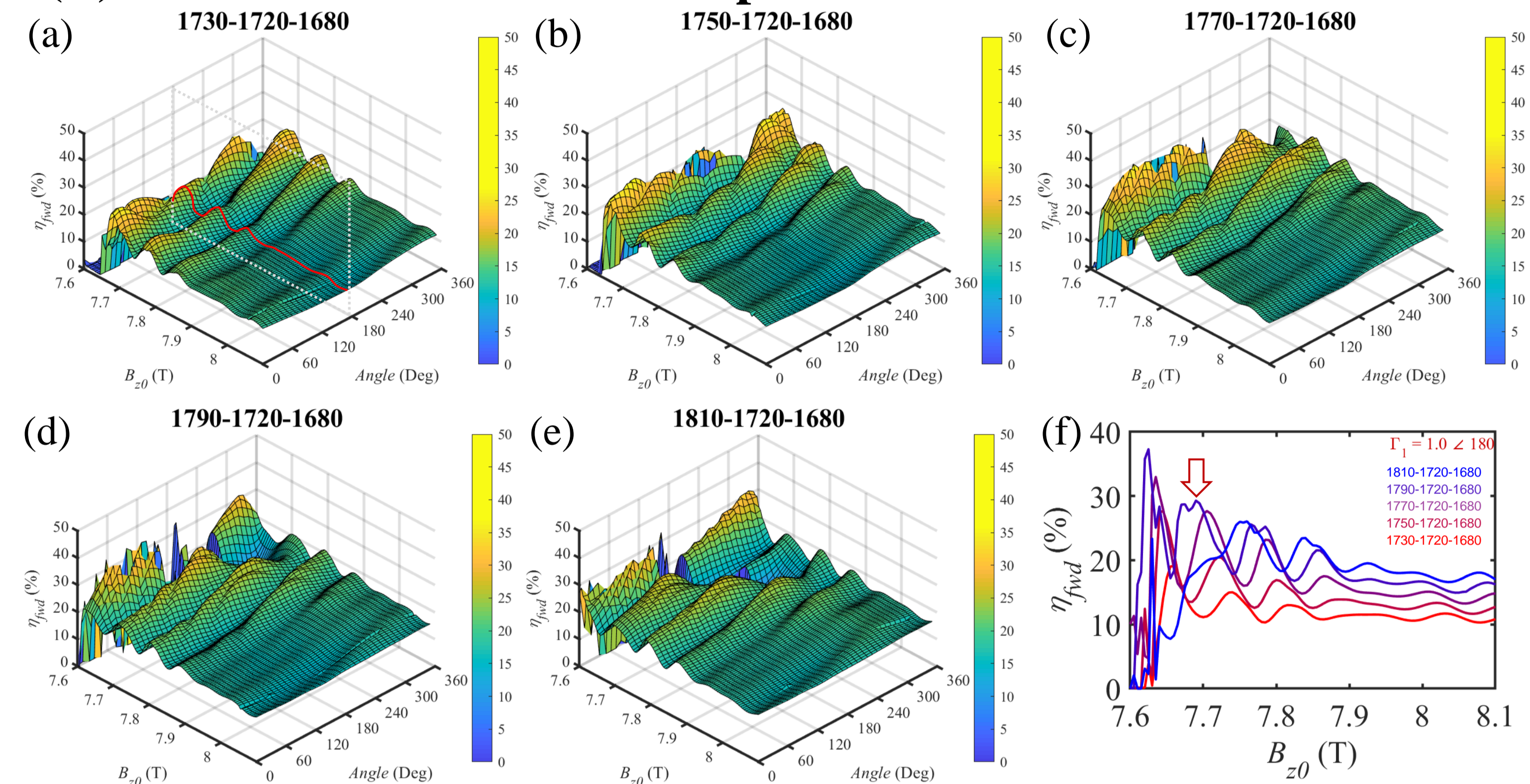


Fig. 4. (a) ~ (e) Simulated output efficiency (η_{fwd}) of Fig.1(b) interaction structure as a function of magnetic field and initial assigned reflection phase ($\Gamma_1 = |1| e^{i\theta}$), the title of each figure is the radius ($r_1 - r_2 - r_3$) in μm . (f) Output efficiency vs magnetic field in different structure, the original structure (1790-1720-1680) is indeed the optimum structure when choosing typical reflection phase (π).

Why Sensitive in reflection phase?

IV. Physical interpretation

(A) Initial mismatch (Δ) (Detuning)

$$\Delta \equiv \omega - k_z v_z - s\Omega_c = \omega - \Omega_{eff} = \Delta\omega$$

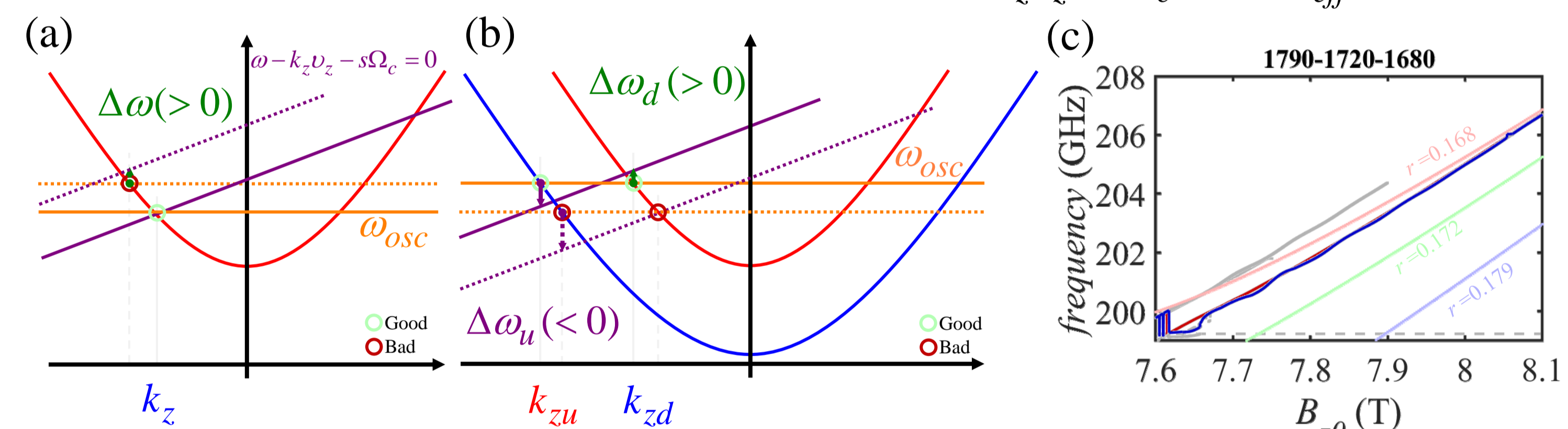


Fig. 5. Dispersion relation for different waveguide radius and beam wave interaction line for different magnetic field. (a) Normal case of dispersion and interaction in uniform waveguide, initial mismatch is slightly larger than zero for positive emission (azimuthal bunching). (b) Larger radius at upstream, higher detuning accelerate the effect phase (ϕ_{eff}) in order to meet the contracted field at a earlier stage of gyro-BWO and compensate the weak interaction at higher magnetic field. (c) Oscillation frequency as a function of magnetic field for two tapered interaction structure, dark blue is reflective gyro-BWO with effective boundary in both side; dark red line is gyro-BWO with Outgoing-wave boundary in both side. Light colored line is the intersection frequency of $r = 0.179$, $r = 0.172$ and $r = 0.168$ respectively.

(B) Reflective Type Gyro-BWO Field Profile

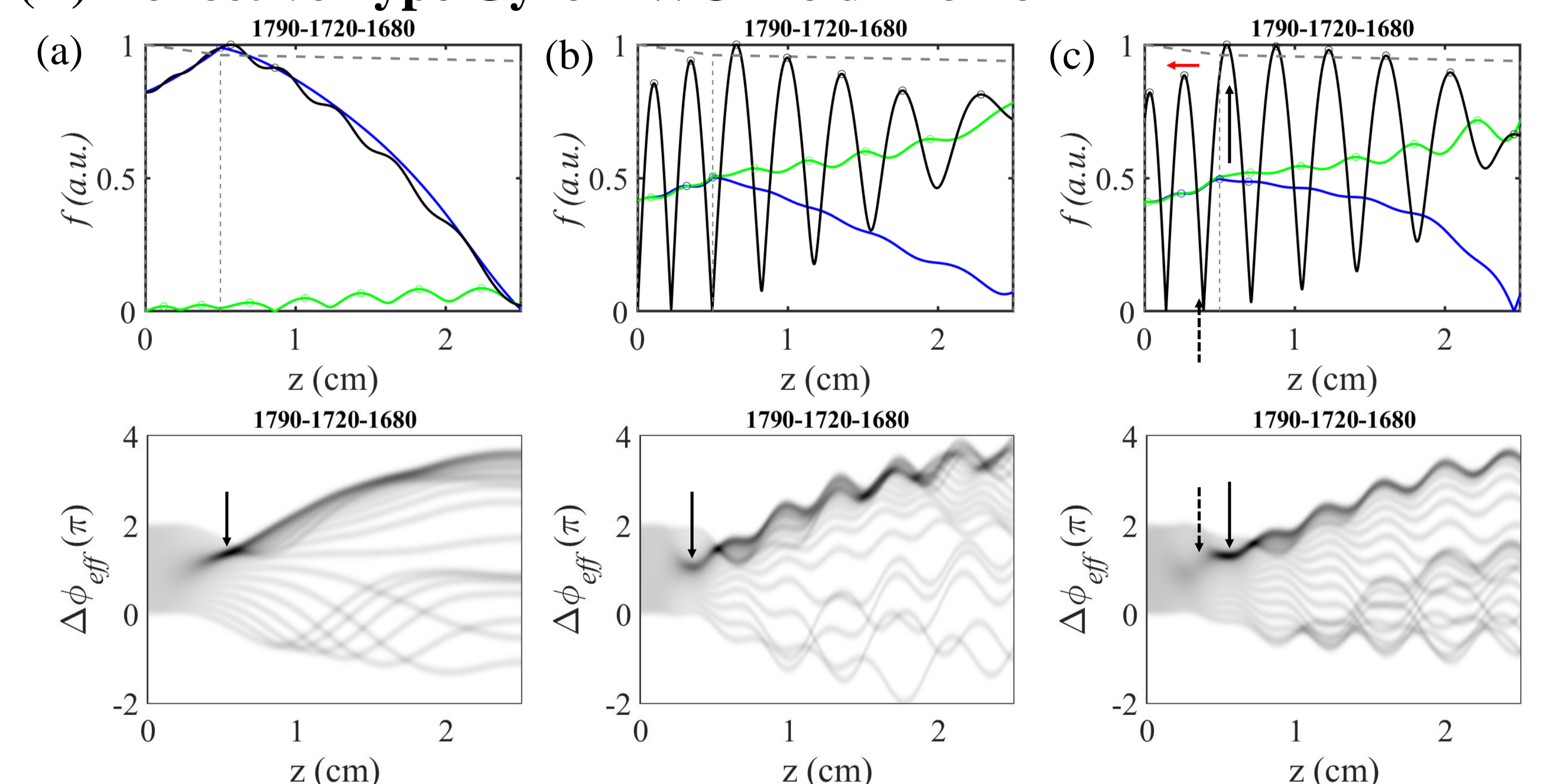


Fig. 6. Field Profile and effect phase as a function of z with $B_{z0} = 7.69$ T. (a) Effective Gyro-BWO with zero reflection at left end. (b) Effective R-gyro-BWO with total reflection phase angle 180 degrees (efficiency=31.54%). (c) Reflection phase angle 300 degrees (efficiency=10.75%).

For R-gyro-BWO, due to standing wave-like field profile, the position where the electron beam bunch is a very important factor affecting the interaction efficiency. This can be seen from the phase and quantity of the electron bunch and the effective interaction length after the bunch is formed.

V. References

N.-C. Chen, T.-H. Chang, C.-P. Yuan, T. Idehara, and I. Ogawa, "Theoretical investigation of a high efficiency and broadband subterahertz gyrotron," Appl. Phys. Lett., vol. 96, no. 16, p. 161503, Apr. 2010.